Journal of Applied Polymer Science

Enhanced Swelling and Methylene Blue Adsorption of Polyacrylamide-Based Superabsorbents Using Alginate Modified Montmorillonite

Haixia Qiu,[1] Zhaoxia Qiu,[2] Jialing Wang,[1] Ruobing Zhang,[1] Fuyuan Zheng[1]
[1]Chemistry Department, School of Science, Tianjin University, Tianjin, People's Republic of China
[2]Jincheng Landscape Research Institute, Jincheng, Shanxi, People's Republic of China
Correspondence to: H. Qiu (E-mail: qhx@tju.edu.cn)

ABSTRACT: Polyacrylamide/sodium alginate modified montmorillonite (PAM/SA-MMT) superabsorbent composites were synthesized by free-radical polymerization under normal atmospheric conditions. They were characterized by X-ray diffraction, scanning electron microscopy, and Fourier transform infrared spectroscopy (FTIR). Their water absorbency and methylene blue (MB) adsorption behaviors were studied. Compared with PAM/MMT composites, PAM/SA-MMT composites demonstrated greater water absorbency (863 g g^{-1} in distilled water and 101 g g^{-1} in 0.9 wt % NaCl solution) and higher adsorption capacity of 2639 mg g^{-1} for MB. The adsorption behaviors of the composites showed that the isotherms and adsorption kinetics were in good agreement with the Langmuir equation and pseudo-second-order equation, respectively. FTIR analysis suggested that the MB adsorption of PAM/SA-MMT composites via a mechanism combined electrostatic, H-bonding and hydrophobic interaction. © 2013 Wiley Periodicals, Inc. J. Appl. Polym. Sci. **2014**, *131*, 40013.

KEYWORDS: gels; adsorption; dyes/pigments; swelling; clay

Received 12 June 2013; accepted 27 September 2013
DOI: 10.1002/app.40013

INTRODUCTION

Superabsorbent polymers (SAPs) are loosely crosslinked hydrophilic polymers capable of absorbing large quantities of water and aqueous fluids in a short time. As the US Department of Agriculture reported the first SAPs,[1] much attention has been drawn to improve their performance in the past several decades. SAPs are widely used in many applications such as hygienic, agriculture, and drug delivery systems.[2] The most common type of SAPs is crosslinked polyacrylic acid. However, conventional SAPs present the drawback of poor water absorbency in saline solutions,[3] which would limit their applications.

Dyes are common water pollutants in wastewater from industries producing fibers, paper, plastics, and so forth. Discharging of dyes into water resources even in small amount can affect the aquatic life.[4] It is difficult to remove dyes from the effluents as most dyes are stable to light and heat and are nonbiodegradable. Methylene blue (MB) is widely used in coloring paper, temporary hair colorant, and dyeing cottons. It can cause many health problems such as eye burns, shock, and heartbeat increase. The treatment of MB-contaminated wastewater is of interest due to its harmful impacts. Until now, several physical, chemical, physicochemical, and biological methods have been explored for treating dyes in wastewater.[5,6] Among them, adsorption has attracted considerable interest due to its economical advantages, low energy input, and easy operation.[7] Activated carbon is the most popular adsorbent and has been widely used for the removal of dyes.[8] However, the application of activated carbon is seriously restricted owing to its high production cost. Consequently, many efforts have been done to find cheaper substitutes such as coal, agricultural wastes, fly ash, silica gel, and clay minerals.[9] However, their adsorption capacity for dyes is limited.

The porous network structure of SAPs allows dye molecules diffusion through them. In recent years, some studies have been reported on the use of SAPs as adsorbents for the adsorption of dyes from aqueous solutions.[10–12] In general, SAPs possess anion functional groups, which can adsorb and trap cationic dyes from wastewaters.

Recently, SAPs composites based on clay, polysaccharides, and synthetic polymers are attracting increasing interest owing to the environmental advantages and practical applications of clay and polysaccharides. However, the reported composites were prepared by graft copolymerization of polysaccharides, vinyl monomers, and clay, which was usually carried out under the

protection of nitrogen.[13–15] Furthermore, there exist only a few reports on the investigation of SAPs incorporated with clay and polysaccharides to improve their dye adsorption properties.[13] It was reported that the organic modification of clay could improve the performance of SAPs/clay composites.[16–18] Inspired by this, we prepared SAPs/clay composites using polysaccharides modified clay, the reaction was carried out under normal atmospheric conditions which caused brevity and simplicity in industrial processes.[19,20]

Sodium alginate (SA), a linear anionic polysaccharide of (1→4)-linked β-D-mannuronic acid and α-L-guluronic acid in a blockwise pattern along the linear chain, is one of the most extensively investigated biopolymers for removal of pollutants such as dyes and heavy metals ions from aqueous solution as it is inexpensive, nontoxic, and efficient.[21] In addition, SA has high affinity for water, the hydrophilic —COO^-Na^+ and —OH groups on SA backbone may improve the water absorbency. According to Zhu et al.,[22] the antisalt ability of polyacrylic acid can be improved by the grafting copolymerization of acrylic acid onto SA, indicating the good salt-resisting property of SA in specific case. Because of its good adsorption capacity and salt-resisting property, SA was chosen as the polysaccharide components and played the role of clay modifier in this study.

Montmorillonite (MMT) is a kind of loose-layer silicate made up of two tetrahedral sheets fused to an edge-shared octahedral sheet of aluminum hydroxide. The incorporation of MMT to SAPs not only reduces production costs but also improves the swelling properties of SAPs.[23,24] In addition, MMT has often been used in the removal of organic dyes due to its high surface area, high cation exchange capacity, and low cost.[25] The introduction of MMT should improve the dye adsorption ability of SAPs.

Polyacrylamide (PAM) is a kind of nonionic polymer. It was chosen as synthetic polymer components because nonionic groups show higher salt resistance than ionic groups. In addition, PAM is relatively low cost compared with polyacrylic acid. To improve its water absorbency and dye adsorption ability, PAM was saponified to transfer a part of —$CONH_2$ groups to COO^-Na^+.

In this work, superabsorbent composites based on PAM and SA-modified MMT were prepared under normal atmospheric conditions, their water absorbency and MB adsorption behaviors were studied. The combination of PAM and SA-modified MMT yields good water absorbency, excellent MB adsorption ability, improved antisalt ability, and relatively low-cost SAPs, which have potential applications in dye removal, agriculture, and hygienic products.

EXPERIMENTAL

Materials

Na^+—MMT (Zhejiang Linan Bentonite Company, China) with a cation exchange capacity of 90 mequiv /100 g was milled through a 300-mesh screen. Acrylamide (AM), sodium hydroxide (NaOH), and sodium chloride (NaCl) were analytical grade and were purchased from Tianjin Chemical Reagent Factory, China. The initiator, potassium persulfate (KPS, analytical grade), and the crosslinker, N,N-methylenebisacrylamide (NMBA, analytical grade), were provided from Tianjin Chemical Reagent Factory, China. SA (analytical grade, viscosity of 1 wt % SA aqueous solution ≥ 0.02 pa s) and MB (analytical grade) were supplied from Shanghai Reagent Company, Shanghai, China. Figure 1 shows the chemical structure of MB. All the chemicals were used without further purification.

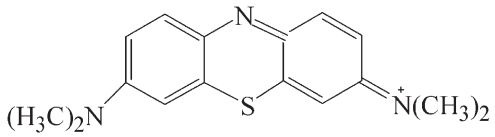

MB

Figure 1. Chemical structure of MB.

Preparation of SA-Modified MMT

A series of SA-modified MMT with different MMT/SA weight ratio were prepared by the following procedure. 1 wt % MMT suspension was prepared in distilled water under stirring conditions for 2 h at room temperature, followed by ultrasonic treatment for 15 min. A certain amount of SA solution (1 wt %) was added to the MMT suspension and stirred vigorously for 2 h at 70°C, the mixture was dried in an oven at 70°C to a constant weight and milled through a 300 mesh screen.

Preparation of PAM/SA-MMT, PAM/MMT, and PAM Superabsorbents

An 8 g AM was dissolved in 32 mL distilled water. Appropriate amount of SA-modified MMT was added to the above monomer solution and stirred vigorously until it was well dispersed. KPS (20 mg + 2.0 mL H_2O) and NMBA (15 mg + 1.5 mL H_2O) were added to the mixed solution of AM and SA-modified MMT. The mixture was stirred and heated to 70°C in a water bath for 2 h, followed by the addition of 10 mL NaOH solution(40 wt %), and then the primary product was heated to 80°C to be saponified for 2 h. After saponification, the product was washed several times with distilled water until pH 7 was achieved. The purified product was dried in an oven at 70°C. The dried gel was milled and screened. All samples used for test had a particle size of 0.2 ~ 0.3 mm. The feed compositions of samples were listed in Table I.

Table I. Feed Composition and Water Absorbency of the SAPs

	Compositions (g)			Water absorption (g/g)	
Sample	AM	MMT	SA	Distilled water	0.9 wt. % NaCl
PAM	8	0	0	552	63
PAM/MMT1	8	0.1	0	527	61
PAM/MMT2	8	0.2	0	359	54
PAM/MMT3	8	0.3	0	332	46
PAM/MMT4	8	0.4	0	302	39
PAM/SA-MMT1	8	0.1	0.2	667	72
PAM/SA-MMT2	8	0.2	0.2	863	101
PAM/SA-MMT3	8	0.3	0.2	743	89
PAM/SA-MMT4	8	0.4	0.2	541	68

The preparation procedure of PAM/MMT composites differed from that of PAM/SA-MMT only in replacing SA-modified MMT with MMT. Similarly, PAM was prepared in the absence of SA-modified MMT.

Measurement of Equilibrium Water Absorbency

The equilibrium swelling (g g^{-1}) was measured according to a conventional tea-bag method.[24] A weighed sample of SAPs (0.10 g) was immersed in 250 mL distilled water or 100 mL 0.9 wt % NaCl solution at room temperature until equilibrium had reached, then the unabsorbed liquid was filtered with a 100-mesh nylon bag, the gel was allowed to drain on a sieve for 10 min, and the bag was weighed to determine the mass of water swollen gel. The water absorption (Q) was calculated using the following equation:

$$Q=(w_2-w_1)/w_1 \quad (1)$$

where w_1 is the mass of dried SAPs and w_2 is the mass of swollen SAPs after absorption.

Adsorption Studies

The MB was made up in stock solution of concentration 5000 mg L^{-1} and was subsequently diluted to the required concentrations. The static-batch studies were performed using 0.10 g (dry weight) of SAPs in 100 mL MB solution with various dye concentrations (100–5000 mg L^{-1}) at 28°C. Removal efficiency (*Re*) and saturated adsorption capacity (q_e) could be obtained according to the following formula:

$$Re(\%)=(C_0-C_e)/C_0\times 100 \quad (2)$$

$$q_e=(C_o-C_e)V/W \quad (3)$$

where C_0 and C_e (mg L^{-1}) are, respectively, the liquid-phase concentrations of MB at initial and equilibrium, V (L) denotes the volume of the solution, and W (g) is the mass of SAPs. The MB concentration in the supernatant was measured by UV–visible spectrophotometer at 663 nm.

For the adsorption kinetics, a weighed sample of SAPs (0.10 g) was immersed in 100 mL of 100 mg L^{-1} MB solution. The test temperature was 28°C. During the adsorption, the MB solution was withdrawn from the adsorption system at indicated times for the analysis of MB concentrations.

Characterization

Wide-angle X-ray diffraction (XRD) measurements were performed with a Japan Rigaka diffractometer using Cu, Ka radiation ($\lambda = 0.154$ nm) at a generator voltage of 40 kV and a generator current of 100 mA. Fourier transform infrared spectroscopy (FTIR) spectra of the samples were recorded on a BIO-RAD FTS3000 IR Spectrum Scanner using KBr pellets. The fracture surfaces of the products were examined using a Philips XL-3 scanning electron microscope.

RESULTS AND DISCUSSION

FTIR and XRD Analysis of SA-Modified MMT

Figure 2 shows the FTIR spectra of MMT, SA, and SA-modified MMT with a MMT/SA weight ratio of 1. In the spectrum of

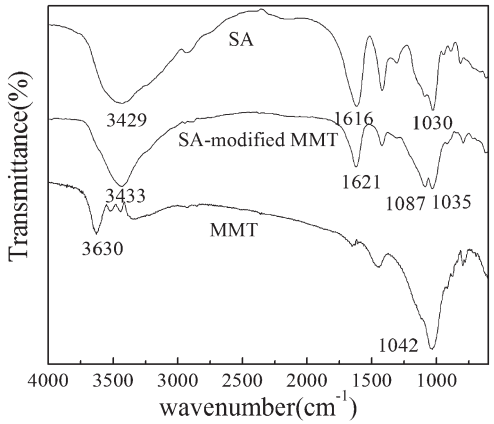

Figure 2. FTIR spectra of MMT, SA, and SA-modified MMT.

SA-modified MMT, the band at 3630 cm^{-1}(—OH stretching of MMT) shifted to lower wavenumber, the band around 1042 cm^{-1}(Si—O—Si stretching of MMT[26]), and the peak at 1030 cm^{-1} (antisymmetric C—O—C stretch of SA[27]) were overlapped and split apart into 1035 and 1087 cm^{-1}, indicating the strong interactions between —OH, Si—O—Si of MMT, and C—O—C of SA. The absorption bands at 1616 cm^{-1}(COO^- stretching) of SA shifted to higher wavenumber at 1621 cm^{-1} in modified MMT, suggesting the slight interactions between COO^- groups of SA and MMT.

XRD analysis is the classical technique that can be used to measure the d (001) spacing of MMT accurately. Increase in the d (001) spacing of MMT has been observed when it is modified with some polysaccharides such as chitosan and carboxymethyl cellulose.[19,20] The XRD patterns of MMT and SA-modified MMT are compared in Figure 3. In the scattering curve of MMT, a prominent peak corresponding to the 001 reflection of MMT occurred at $2\theta = 7.07°$, using Bragg's equation, an average basal spacing of 1.25 nm was calculated for this reflection. The 001 peak was observed in SA-modified MMT and its peak position remained unchanged, but the peak became much broader. Because the intercalation of modifiers to MMT layers leads to a shift of 001 peak to smaller angles,[28] no shift of the 001 peak to smaller angles indicated that SA did not intercalate into the stacked MMT galleries, and the reaction between SA and MMT

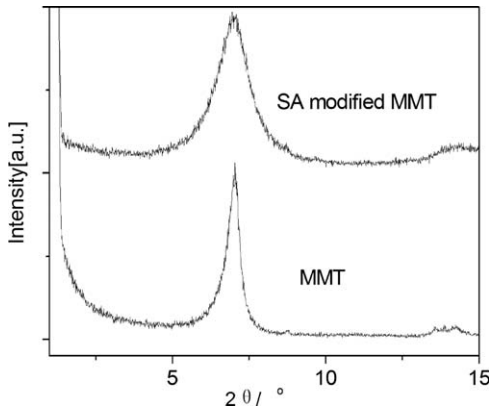

Figure 3. XRD patterns of MMT and SA-modified MMT.

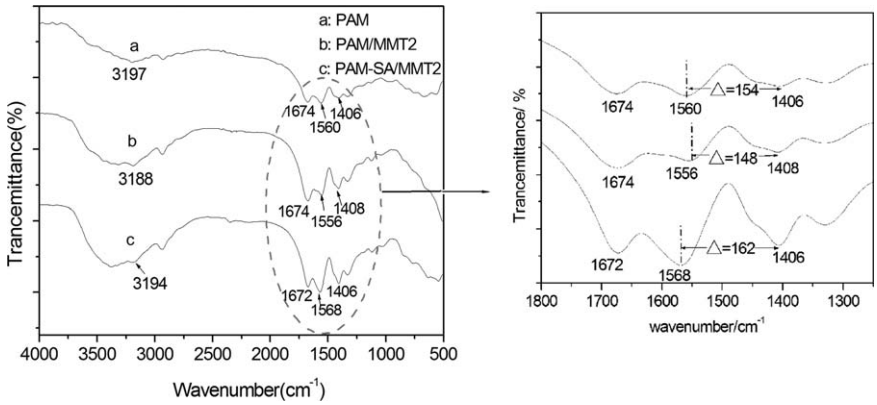

Figure 4. FTIR spectra of PAM, PAM/MMT2, and PAM/SA-MMT2.

occurred on the external surfaces of MMT particles. It is reported that the irregular arrangement of MMT layers results in a broad XRD patterns,[29] broadening of 001 peak observed in SA-modified MMT reflected a lower degree of ordering for MMT layers compared with pristine MMT.

Effect of SA-Modified MMT on Water Absorbency

Table I shows that the water absorbency of PAM/MMT composites decreased with the increase of MMT content. It can be observed that the water absorbency of the PAM/SA-MMT composites was higher than that of the corresponding PAM/MMT composites, for example, the water absorbency of PAM/SA-MMT2 was 863 g g^{-1}, while that of PAM/MMT2 was only 359 g g^{-1}.

The decreased water absorbency of PAM/MMT composites at high MMT content can be due to the formation of additional physical crosslinking points between MMT particles and the PAM matrix, this behavior has been reported in a variety of SAPs/MMT composites.[30,31] We postulated that the additional physical crosslinking points between MMT and PAM matrix were effectively suppressed in PAM/SA-MMT composites, which was one of the reasons that caused great water absorbency difference between PAM/MMT2 and PAM/SA-MMT2 composites. This hypothesis can be can be evidenced from FTIR spectrum.

In the FTIR spectrum of PAM/MMT2 (Figure 4, curve b), bands around 1042 cm^{-1} (Si—O—Si stretching) and 3630 cm^{-1} (—OH stretching) of MMT (Figure 1) disappeared; a peak at 1560 cm^{-1} corresponding to —COO^- of PAM (Figure 4, curve a) shifted to low frequency at 1556 cm^{-1}; the splitting Δ between asymmetric and symmetric —COO^- frequencies, which is related to the nature of the carboxylate coordination,[32,33] decreased from 154 cm^{-1} of PAM to 148 cm^{-1}. FTIR analysis indicated the interaction between —OH, Si—O—Si of MMT, and —COO^- of PAM. These interactions (denoted as PAM-MMT interactions) could cause high physical crosslinking density and consequently low water absorbency.

The FTIR analysis of PAM/MMT2 and modified MMT (discussed above) demonstrated that Si—O—Si and —OH groups were the active sites of MMT in both PAM-MMT interactions and SA-MMT interactions, so the preformed SA-MMT interactions in modified MMT might consume most of the active sites of MMT, resulting in the suppression of PAM-MMT interactions in PAM/SA-MMT2.

In the spectrum of PAM/SA-MMT2 (Figure 4, curve c), the peak at 1556 cm^{-1} of PAM/MMT2(COO^- stretching, related to PAM-MMT interactions) shifted to higher wavenumber at 1568 cm^{-1}; the relative intensities of —C═O deformation (1672 ~ 1674 $cm^{-1)}$ and COO^- stretching changed dramatically(for PAM/MMT, the intensity of —C═O is higher than COO^- stretching at 1556 cm^{-1}, while for PAM/SA-MMT2, the former is much lower than the later at 1568 cm^{-1}), indicating an effective inhibition of PAM-MMT interactions due to the modification of MMT. Moreover, the splitting Δ between the asymmetric and symmetric —COO^- frequencies increased from 148 cm^{-1} of PAM/MMT to 162 cm^{-1}, suggesting the bonding mechanisms of —COO^- to MMT is quite different in these two composites(it is possible to discriminate between different bonding mechanisms by measuring the splitting Δ[34]), which further confirmed the effective inhibition of PAM-MMT interactions. As a result, the physical crosslinking points originated from PAM-MMT interactions would decrease in PAM/SA-MMT2, and consequently its water absorbency increased. The schematic preparation of PAM-SA/MMT superabsorbent composites is shown in Figure 5.

Other reasons that cause the great water absorbency difference between PAM/MMT2 and PAM/SA-MMT2 composites are as follows: (i) The ionic COO^- groups of SA could increase the ionizability and ionic charge content of MMT surfaces. Therefore, swelling capacity is enhanced by expansion of the network promoted by the chain expansion. (ii) The dispersion degree of clay particles in the polymer matrix is important for obtaining SAPs/clay composites with high water absorbency.[30,31] Dispersed MMT particles might be stabilized by electrostatic repulsion between carboxylate anions of the SA adsorbed. Thereafter, MMT dispersed homogenously in the composite, which can be evidenced from the scanning electron microscopy (SEM) images (Figures 6 and 7).

The white particles in the SEM images correspond to MMT, and the black background represents the polymer matrices. Figure 6 reveals that the typical sizes of MMT particles were in the range of 0.1 ~ 0.25 μm and dispersed homogenously in PAM/SA-MMT2 composite, while in PAM/MMT2

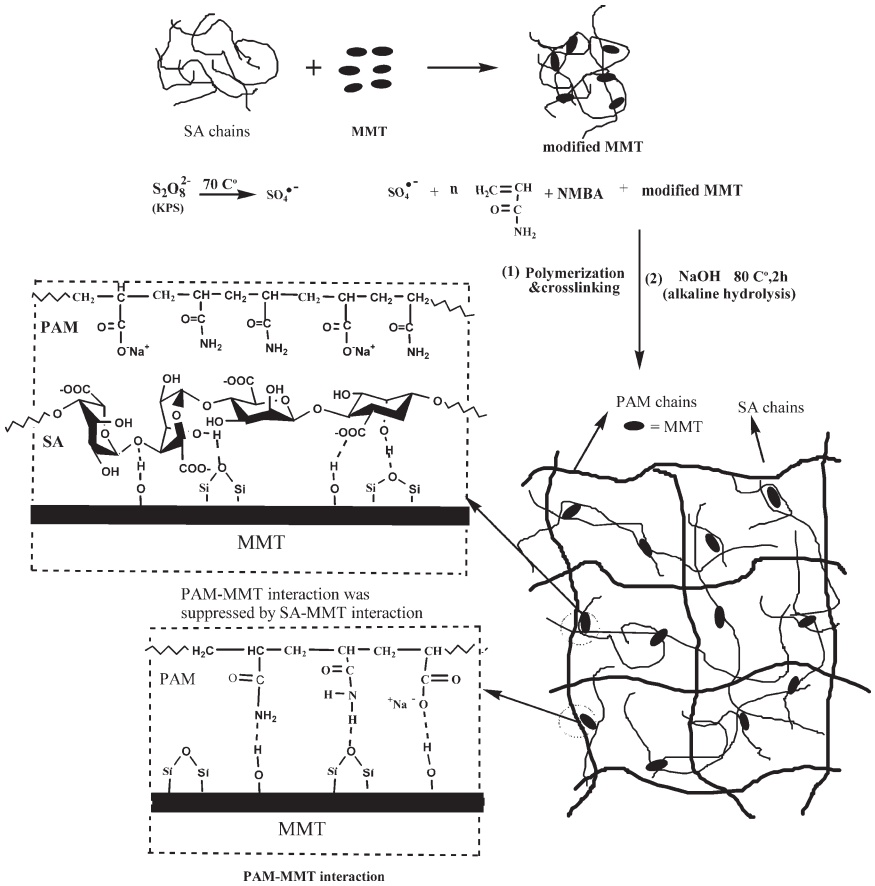

Figure 5. Schematic preparation of PAM-SA/MMT superabsorbent composites.

composite (Figure 7), MMT particles were very widely dispersed (0.25 ∼ 1.25 μm) and the agglomeration of MMT particles can be observed, indicating that SA-modified MMT can be dispersed better than can pristine MMT in a hydrophilic polymer.

Effect of MMT/SA Weight Ratio on Water Absorbency

PAM/SA-MMT composites with different MMT/SA weight ratio are illustrated in Table I, sample PAM/SA-MMT1 ∼ PAM/SA–MMT4. The results show that the water absorbency of the composites increased by increasing the MMT/SA weight ratio up to 1 and then decreased with any further increase. At low MMT/SA weight ratio (<1), the amount of SA was more than that of MMT, the extra SA chains might entangle with PAM chains, which would inhibit the water adsorption capacity. At high MMT/SA weight ratio (>1), the amount of MMT was more than that of SA, so some of the active sites of MMT were not consumed by SA, as a result, PAM-MMT interactions could not be prevented and the corresponding physical crosslink points became higher, which would decrease the water absorbency.

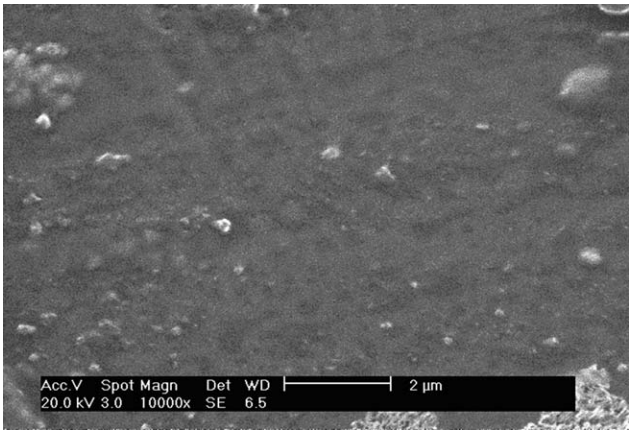

Figure 6. SEM of PAM/SA-MMT2.

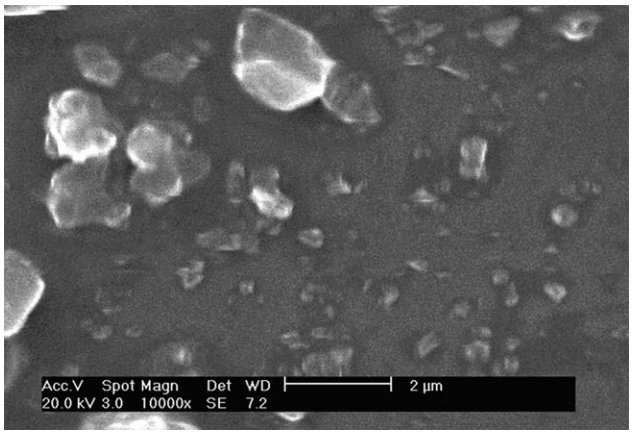

Figure 7. SEM of PAM/MMT2.

Table II. Effect of Initial MB Concentration on MB Adsorption, Percentage Dye Removal, and Water Absorbency of PAM/MMT2 and PAM/SA-MMT2 Composites

	PAM/MMT2			PAM/SA-MMT2		
Initial MB concentration (mg/L)	q_m (mg/g)	*Re* (%)	Water absorbency in MB solution (g/g)	q_m (mg/g)	*Re* (%)	Water absorbency in MB solution (g/g)
100	93.2	93.2	268	98.1	98.1	302
500	430.2	86.0	83	489.3	97.8	117
1000	826.8	82.7	31	943.3	94.3	65

Effect of Ion Strength on Water Absorbency

Salt resistance of SAPs, the ability to absorb liquids in salt solutions, is an important aspect in many applications, such as horticulture and personal hygiene products. As shown in Table I, the water absorbency of the SAPs sharply decreased in 0.9 wt % NaCl solution. This known phenomenon has been attributed to the reduction of osmotic pressure difference between the polymeric network and the external saline solution. The penetration of counter ions (Na^+) into the anionic polymeric network makes the screening effect of them on hydrophilic groups (—COO^-) more evident, which also decreases water absorbency of the SAPs.

Table I shows that the water absorbency of PAM/SA-MMT composites in 0.9 wt % NaCl solution was higher than those of PAM and PAM/MMT, reaching 101 g g^{-1}. SA has good salt-resisting property in specific case,[22] the modification of MMT with SA benefits the improvement of the PAM polymeric network and consequently the salt-resistant property of SA may be shown. In addition, this antisalt behavior may be due to the coeffect contribution of nonionic groups such as —$CONH_2$ from PAM and —OH from SA (or MMT).

Effect of SA-Modified MMT on MB Adsorption

The q_m and *Re* of PAM/MMT2 and PAM-SA/MMT2 composites at various initial MB concentrations are presented in Table II. PAM/SA-MMT2 showed much higher q_m and *Re*% than PAM/MMT2, indicating that the modification of MMT has a significant effect on the MB adsorption properties. As discussed above, the modification of MMT effectively destroyed the PAM-MMT interactions in PAM/SA-MMT2 composite, which ultimately enhanced free volume and hence number of binding sites per unit volume of the composite. Moreover, PAM/SA-MMT2 has higher swelling capacity in MB solution than PAM/MMT2 (Table II), and consequently its network is sufficiently expanded. The expanded network of the adsorbent favors the interaction between the cationic dye molecules and the adsorption sites on the adsorbent surface.[35] In addition, the anionic groups (COO^-) on SA macromolecules can offer adsorption sites for cationic MB dye absorption.

As shown in Table II, the adsorption capacity increased with increasing initial MB concentrations for both composites. This could be explained by the fact that with increasing MB content in the initial solution, concentration gradients at the composite-solvent interfaces could take place causing an enhancement of the MB adsorption.[36] It can be observed that the adsorption capacity difference between the two composites increased with increasing MB concentration. The difference increased from 4.9 to 116.5 mg g^{-1} when MB concentration increased from 100 to 1000 mg L^{-1}. In addition, PAM/SA-MMT2 showed higher *Re*% than PAM/MMT2 with the MB concentration ranging from 100 to 1000 mg L^{-1}. In solution with 1000 mg L^{-1} of MB, the *Re*% was 94.3% for PAM/SA-MMT2, in case of PAM/MMT2 composites, there was a lower *Re*% of 82.7%. The above results indicate the good adsorption ability of PAM/SA-MMT composite in high-concentration MB solution.

Effect of Ion Strength on MB Adsorption

Apart from the dyes, wastewater from dye-producing industries often contains metal ions such as Na^+, K^+, and Ca^{2+}. The presence of metal ions leads to high ionic strength, which may significantly affect the performance of adsorption process. In theory, increasing ion strength will decrease adsorption capacity when there is the electrostatic attraction between the adsorbent surface and adsorbate ions.[37] NaCl is frequently used as a stimulator in dyeing process. Figure 8 shows the effect of NaCl concentration on MB adsorption and indicates that PAM/SA-MMT2 shows higher q_m than PAM/MMT2 in the NaCl concentration examined. PAM/SA-MMT2 composite exhibited higher swelling ability in NaCl solution than PAM/MMT2 (Table I), consequently, it has a relatively expanded network compared with PAM/MMT2, which favors the interaction between the MB molecules and the adsorption sites on the composite surface.

Adsorption Isotherms

Adsorption isotherms are important for the description of how adsorbates will interact with an adsorbent, and are vital to the

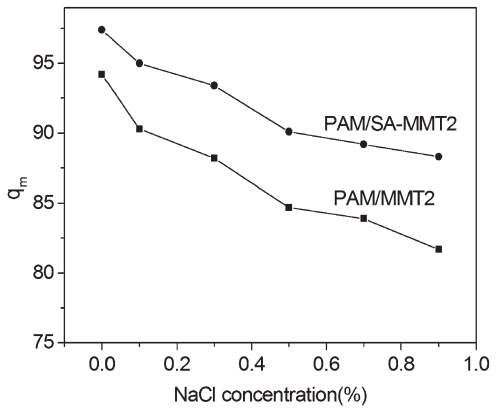

Figure 8. Effect of ion strength on MB adsorption experiments (MB concentration: 100 mg L^{-1})

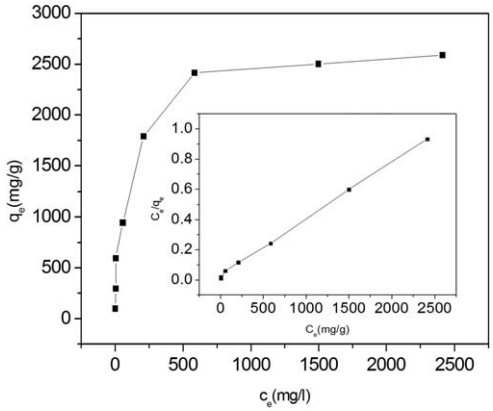

Figure 9. Adsorption isotherms of MB on PAM/SA-MMT2 (The inset shows Langmuir plot of PAM/SA-MMT2 with MB).

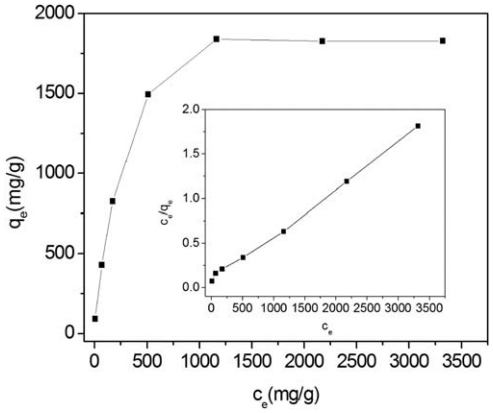

Figure 10. Adsorption isotherms of MB on PAM/MMT2 (The inset shows Langmuir plot of PAM/MMT2 with MB).

design of adsorption systems. The most widely used isotherm models are Langmuir and Freundlich models.

The Langmuir adsorption model describes monolayer adsorption of adsorbate onto a homogeneous adsorbent surface. Moreover, there are negligible interactions between the adsorbed molecules and adsorption sites having uniform energies. The Langmuir equation is described by the following equation[38]:

$$\frac{C_e}{q_e} = \frac{C_e}{q_m} + \frac{1}{bq_m} \tag{4}$$

where C_e (mg L^{-1}) denotes the equilibrium concentration in the solution, q_e (mg g^{-1}) is the amount of MB adsorbed per unit weight of adsorbents at specified equilibrium, q_m (mg g^{-1}) is the maximum adsorption at monolayer coverage, and b (L mg^{-1}) represents the Langmuir constant related to the free energy or net enthalpy of adsorption. q_m and b can be calculated from the slope and the intercept of the linear plot.

The Freundlich equation is an empirical model based on adsorption on a heterogeneous surface. The linear form of the Freundlich equation is[39]:

$$\log q_e = \log k + \frac{1}{n}\log C_e \tag{5}$$

where q_e (mg g^{-1})is the amount adsorbed at equilibrium, C_e (mg L^{-1}) is the equilibrium concentration of the MB, k is a Freundlich constant representing the adsorption capacity, and n represents a constant depicting the adsorption intensity. k and n are determined from the intercept and slope of linear plot of $\log q_e$ against $\log C_e$, respectively.

Figures 9 and 10 show the adsorption isotherm of MB on PAM/SA-MMT2 and PAM/MMT2, respectively. Data from the adsorption isotherm were evaluated by Langmuir and Freundlich adsorption models, and the isotherm parameters and correlation coefficient R^2 were summarized in Table III. On comparing the R^2, it is concluded that both of the two composites were better fitted into the Langmuir model than the

Table III. Isotherm Parameters for MB Adsorption onto PAM/MMT2 and PAM/SA-MMT2 Composites

	Langmuir			Freundlich		
Sample	q_m (mg/g)	b (L/mg)	R^2	k	n	R^2
PAM/MMT2	1954	0.00572	0.9987	48.94	2.02	0.9343
PAM/SA-MMT2	2639	0.0159	0.9994	152.05	2.45	0.9392

Table IV. Comparison of Recent Reported Adsorption Capacities of MB on SAPs

Adsorbent	Q_{max} (mg/g)	Isotherms model	Reference
PAM/SA-MMT	2639	Langmuir	This work
Poly(N,N-dimethylacrylamide-co-sodium acrylate)	800	Langmuir	[41]
Chitosan-g-poly (acrylic acid)/MMT	1859	Langmuir	[13]
Hydrogel composites based on attapulgite	1979.48	Langmuir	[42]
Lignocellulose-g-poly(acrylic acid)/montmorillonite	1994.38	Langmuir	[43]
Poly(2-acrylamido-2-methylpropane sulfonic Acid-co-itaconic acid)	1000	Langmuir	[44]

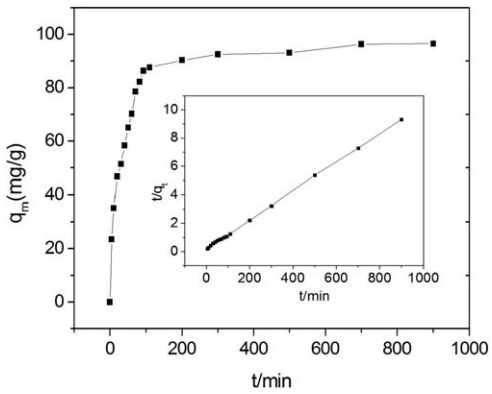

Figure 11. Kinetic adsorption results of MB on PAM/SA-MMT2 (The inset figure shows Pseudo-second-order model for the adsorption of MB on PAM/SA-MMT2).

Freundlich model (Langmuir isotherms for PAM/SA-MMT2 and PAM/MMT2 are presented in the inset of Figures 9 and 10, respectively). This suggests that the adsorption of MB by the two composites involves monolayer adsorption rather than multilayer adsorption, and the adsorbed MB molecules do not interact or compete with each other.

The fitness of experimental data to Langmuir isotherm equation indicated the homogeneous nature of the composite surface. The *b* values (Langmuir constant) related to sorption energy, the higher *b*, the higher is the affinity of the adsorbent for the adsorbate.[40] As listed in Table III, the *b* value of PAM/SA-MMT2 (0.0159 L mg^{-1}) is much higher than that of PAM/MMT2 (0.00572 L mg^{-1}), indicating the higher binding energy of PAM/SA-MMT2 compare with PAM/MMT2. The maximum adsorption capacity of PAM/SA-MMT2 (2639 mg g^{-1}) is considerably higher than those of PAM/MMT (1954 mg g^{-1}) and other reported hydrogel adsorbents (Table IV).

Adsorption Kinetics

Figure 11 shows the kinetic adsorption results of MB on PAM/SA-MMT2 composite. The initial slope of the curve represents the adsorption rates. High adsorption rate was observed at the beginning and a plateau was gradually reached thereafter. To investigate the mechanism of sorption and the rate constant for the adsorption of MB on PAM/SA-MMT2 composite, pseudo-second-order rate models was used. The pseudo-second-order equation was given below[45]:

$$\frac{t}{q_t} = \frac{1}{kq_e^2} + \frac{t}{q_e} \tag{6}$$

where q_e and q_t (mg g^{-1}) are the amounts of dye adsorbed at equilibrium and at time *t* (min), respectively, and k_1 (min^{-1}) is the rate constant of adsorption.

The inset in Figure 11 shows the pseudo-second-order model for the adsorption of MB on PAM/SA-MMT2. The R^2 value of the second-order rate model was 0.9998, suggesting that the adsorption of MB on PAM/SA-MMT2 may be best described by the pseudo-second-order kinetic model, which was based on the assumption that the rate-limiting step may be chemical sorption involving valence forces through sharing or exchange electrons between adsorbent and adsorbate.[46]

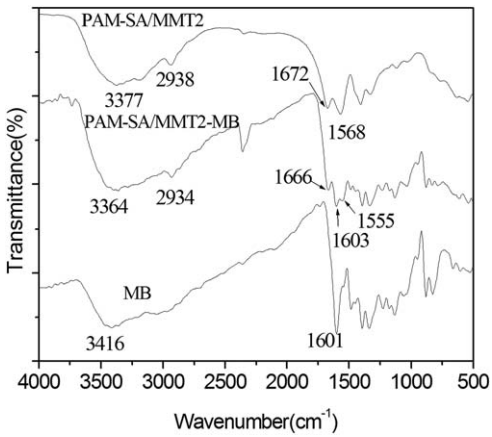

Figure 12. FTIR spectra of PAM/SA-MMT2, MB, and PAM/SA-MMT2-MB systems.

FTIR Analysis of PAM/SA-MMT Composites after Adsorption

To examine the nature of interactions between MB and PAM/SA-MMT composites, FTIR spectra of PAM/SA-MMT2, MB, and PAM/SA-MMT2-MB are compared in Figure 12.

After the adsorption, —OH stretching mode of PAM/SA-MMT2 shifted from 3377 cm^{-1} to lower wavenumbers at 3364 cm^{-1}, indicating the formation of hydrogen bonding between MB and the —OH groups of MMT (or SA); the vibration band of $—CONH_2$ shifted from 1672 cm^{-1} to lower wavenumber at 1666 cm^{-1}, showing the H-bonding between MB and $—CONH_2$ of PAM; the $—COO^-$ vibration band at 1568 cm^{-1} of PAM was split apart into 1555 and 1603cm^{-1}, suggesting the strong electrostatic interaction between MB and $—COO^-$ groups; the movement of methylene vibration from 2938 to 2934 cm^{-1} indicated that adsorption of MB onto PAM/SA-MMT2 might involve some hydrophobic interactions. Based on above discussion, it could be presumed that the MB adsorption on PAM/SA-MMT composites via a mechanism combined electrostatic, H-bonding and hydrophobic interaction, which is in agreement with the cationic dye adsorption on other superabsorbent composites based on MMT.[47,48]

CONCLUSIONS

A novel superabsorbent composite based on PAM and SA-modified MMT was prepared by aqueous solution polymerization under normal atmospheric conditions. Owing to the modification of MMT, the resulting composite showed higher swelling capacity, salt-resisting ability, and MB absorption capacity (especially in saline and high-concentration MB solutions) as compared with PAM/MMT composite. Adsorption isotherm study suggested that MB adsorption on PAM/SA-MMT composites best followed the Langmuir isotherm model. Kinetic data of adsorption was well fitted by the pseudo-second-order kinetic model. FTIR spectra showed that the MB adsorption of the composite via a mechanism combined electrostatic, H-bonding and hydrophobic interaction. The excellent MB

adsorption capacities, water absorbency, antisalt ability, and relatively low cost make the composite very useful for applications in wastewater treatment and agriculture.

ACKNOWLEDGMENTS

We gratefully acknowledge financial support from the following agencies: Science and Technology Program of Shanxi Province (Grant No. 20110311017-7) and Science and Technology Development Program of Jincheng, Shanxi Province (Grant No. 201002065).

REFERENCES

1. Fanta, G. F.; Burr, R. C.; Rusell, C. R.; Rist, C. E. *J. Polym. Sci. Polym. Chem.* **1969**, *7*, 1675.
2. Zohuriaan-Mehr, M. J.; Omidian, H.; Doroudiani, S.; Kabiri, K. *J. Mater. Sci.* **2010**, *45*, 5711.
3. Bahaj, H.; Benaddi, R.; Bakass, M.; Bayane, C. *J. Appl. Polym. Sci.* **2010**, *115*, 2479.
4. Walker, G. M.; Hansen, L.; Hanna, L. A.; Allen, S. *J. Water Res.* **2003**, *37*, 2081.
5. Verma, A. K.; Dash, R. R.; Bhunia, P. *J. Environ. Manage.* **2012**, *93*, 154.
6. Singh, K.; Arora, S. *Crit. Rev. Environ. Sci. Technol.* **2011**, *41*, 807.
7. Silva, J. P.; Sousa, S.; Rodrigues, J.; Antunes, H.; Porter, J. J.; Goncalves, I.; Ferreira-Dias, S. *Sep. Purif. Technol.* **2004**, *40*, 309.
8. Demirbas, A. *J. Hazard. Mater.* **2009**, *167*, 1.
9. Rafatullah, M.; Sulaiman, O.; Hashim, R.; Ahmad, A. *J. Hazard. Mater.* **2010**, *177*, 70.
10. Şolpan, D.; Torun, M.; Güven, O. *J. Appl. Polym. Sci.* **2008**, *108*, 3787.
11. Mahdavinia, G. R.; Massoumi, B.; Jalili, K.; Kiani, G. *J. Polym. Res.* **2012**, *19*, 9947.
12. Neelesh, B. S.; Giridhar, M. *J. Appl. Polym. Sci.* **2012**, *124*, 3892.
13. Wang, L.; Zhang, J. P.; Wang, A. Q. *Colloids Surf. A* **2008**, *322*, 47.
14. Al, E.; Guclu, G.; Iyim, T. B.; Emik, S.; Özgümüş, S. *J. Appl. Polym. Sci.* **2008**, *109*, 16.
15. Nakason, C.; Wohmang, T.; Kaesaman, A.; Kiatkamjornwong, S. *Carbohydr. Polym.* **2010**, *81*, 348.
16. Zheng, L. C.; Xu, S. M.; Peng, Y.; Wang, J. D.; Peng, G. *Polym. Adv. Technol.* **2007**, *18*, 194.
17. Xu, S. M.; Zhang, S. F.; Yang, J. Z. *Mater. Lett.* **2008**, *62*, 3999.
18. Marandi, G. B.; Sharifnia, N.; Hosseinzadeh, H. *J. Appl. Polym. Sci.* **2006**, *101*, 2927.
19. Qiu, H. X.; Yu, J. G.; Zhu, J. L. *Polym. Polym. Compos.* **2005**, *13*, 167.
20. Qiu, H. X.; Yu, J. G. *J. Appl. Polym. Sci.* **2008**, *107*, 118.
21. Rocher, V.; Bee, A.; Siaugue, J. M.; Cabuil, V. *J. Hazard. Mater.* **2010**, *178*, 434.
22. Zhu, Y. B.; Pu, B. Y.; Zhang, J. L.; Shen, J. C. *J. Appl. Polym. Sci.* **2001**, *79*, 572.
23. Lee, W. F.; Yang, L. G. *J. Appl. Polym. Sci.* **2004**, *92*, 3422.
24. Xiang, Y. Q.; Peng, Z. Q.; Chen, D. *J. Eur. Polym. J.* **2006**, *42*, 2125.
25. Klika, Z.; Pustkova, P.; Dudova, M. *Clay Miner.* **2011**, *46*, 461.
26. Wu, J. H.; Lin, J. M.; Zhou, M.; Wei, C. *Macromol. Rapid Commun.* **2000**, *21*, 1032.
27. Pongjanyakul, T.; Priprem, A.; Puttipipatkhachorn, S. *J. Controlled Release* **2005**, *107*, 343.
28. Ray, S. S.; Okamoto, M. *Prog. Polym. Sci.* **2003**, *28*, 1539.
29. Fukushima, Y. *Clays Clay Miner.* **1984**, *32*, 320.
30. Kabiri, K.; Zohuriaan-Mehr, M. *J. Polym. Adv. Technol.* **2003**, *14*, 438.
31. Lin, J. M.; Wu, J. H.; Yang, Z. F.; Pu, M. L. *Macromol. Rapid Commun.* **2001**, *22*, 422.
32. Deacon, G. B.; Phillips, R. *J. Coord. Chem. Rev.* **1980**, *33*, 227.
33. Pajtasova, M.; Ondrusova, D.; Jona, E.; Mojumdar, S. C.; L'alikova, S.; Bazylakova, T.; Gregor, M. *J. Therm. Anal. Calorim.* **2010**, *100*, 769.
34. Kirwan, L. J.; Fawell, P. D.; van Bronswijk, W. *Langmuir* **2003**, *19*, 5802.
35. Anirudhan, T. S.; Suchithra, P. S.; Radhakrishnan, P. G. *Appl. Clay Sci.* **2009**, *43*, 336.
36. Paulino, A. T.; Guilherme, M. R.; Reis, A. V. *J. Colloid Interface Sci.* **2006**, *301*, 55.
37. Al-Degs, Y. S.; El-Barghouthi, M. I.; El-Sheikh, A. H.; Walker, G. M. *Dyes Pigm.* **2008**, *77*, 16.
38. Behnamfard, A.; Salarirad, M. M. *J. Hazard. Mater.* **2009**, *170*, 127.
39. Zhou, L.; Zhang, J. H.; Zhou, Y. *Langmuir* **2001**, *17*, 5503.
40. Ma, B.; Oh, S.; Shin, W. S.; Choi, S. *J. Desalination* **2011**, *276*, 336.
41. Bekiari, V.; Sotiropoulou, M.; Bokias, G.; Lianos, P. *Colloids Surf. A.* **2008**, *312*, 214..
42. Liu, Y.; Wang, W. B.; Jin, Y. L.; Wang, A. Q. *Sep. Sci. Technol.* **2011**, *46*, 858.
43. Shi, Y. R.; Xue, Z. H.; Wang, X. M.; Wang, L.; Wang, A. Q. *Polym. Bull.* **2013**, *70*, 1163.
44. Coskun, R.; Delibas, A. *Polym. Bull.* **2012**, *68*, 1889.
45. Ho, Y. S.; McKay, G. *Process Biochem.* **1999**, *34*, 451.
46. Bulut, E.; Özaca, M.; Şengil, İ. A. *Microporous Mesoporous Mater.* **2008**, *115*, 234.
47. Abdel-Aziz, H. M.; El-Zahhar, A. A.; Siyam, T. *J. Appl. Polym. Sci.* **2012**, *124*, 386.
48. Kundakci, S.; Uzum, O. B.; Karadag, E. *React. Funct. Polym.* **2008**, *68*, 458.